Eur. Phys. J. D (2005)
DOI: 10.1140/epjd/e2005-00219-1

THE EUROPEAN PHYSICAL JOURNAL D

Stability of a single vortex in a trapped Bose-Einstein condensate

G.M. Kavoulakis[a]

Mathematical Physics, Lund Institute of Technology, P.O. Box 118, 22100 Lund, Sweden

Received 3 January 2005 / Received in final form 11 May 2005
Published online 9 August 2005 –

Abstract. We investigate the lowest state of a Bose-Einstein condensate with an off-center vortex state that is confined in a rotating harmonic potential. Our results are consistent with the fact that any single off-center vortex is unstable. Furthermore, a vortex state located at the center of the cloud first becomes locally stable as the rotational frequency increases. Finally our study implies the existence of hysteresis effects.

PACS. 03.75.Kk Dynamic properties of condensates; collective and hydrodynamic excitations, superfluid flow

1 Introduction

When rotated, a superfluid forms quantized vortex states. Numerous studies have examined in the past vortices in the traditional superfluid liquid helium-IV. Recently in some remarkable experiments vortices have also been created and observed in vapors of trapped ultracold atoms [1–4].

One of the basic questions in atomic systems is the formation and stability of vortex states. Because of the confinement (which is typically harmonic), there is a number of differences as compared to homogeneous superfluids. For example, the energy spectrum is discreet, the density is inhomogeneous and finally for harmonic confinement the frequency of rotation of the gas is limited by the trap frequency.

Many studies have examined the physics of vortices in trapped gases [5–16]. The basic picture is that above a critical frequency of rotation of the trap, one vortex state forms in the gas, while as the rotational frequency increases further, more vortices enter the cloud, eventually forming an array. One of the most fundamental and important questions is thus the way that the first vortex state forms.

In the present study we develop a method which allows us to examine this problem in the limit of weak interactions, where the typical atom-atom interaction energy is smaller than the oscillator quantum of energy and one can restrict himself to the subspace of states in the lowest Landau level. In this limit the gas has a very peculiar property when the angular momentum per atom ranges between zero and unity, as the interaction energy scales linearly with the angular momentum [14,17–20], just like as in an ideal gas. This is an exact result within the lowest Landau level subspace of states. The linear behavior of the spectrum has important implications on the rotational properties of the gas, as at a critical frequency of rotation which is smaller than the trap frequency by a (small) amount that is proportional to the ratio between the interaction energy and the oscillator energy, the gas is predicted to undergo a discontinuous phase transition from the non-rotating state to a state with one vortex at the center of the trap [14].

However, as we show below, inclusion of states beyond the ones in the lowest Landau level implies that the energy of the gas does not increase linearly with the angular momentum in general. In the present study we use second-order perturbation theory to calculate the lowest-order correction, for which the energy is no longer linear and from the derived dispersion relation we identify the minima of the energy of the gas in the rotating frame, for a given rotational frequency of the trap Ω. Given this calculation, we then analyse the rotational behavior of the cloud.

Our study suggests that any single off-center vortex state is unstable. Furthermore, a vortex state that is located at the center of the cloud first becomes locally stable. We also predict that the gas comes to rest at a smaller Ω than the one where rotation sets in (see Fig. 1), and the system exhibits hysteresis [15], which is a general characteristic of first-order phase transitions. The graphs in Figure 1 show schematically the energy of the gas in the rotating frame for certain physically-relevant rotational frequencies which we calculate below.

The importance of our study is multifold: first of all, it provides insight on the stability of a single vortex in confined gases of atoms. Although this is one of the most fundamental questions in the field of cold atoms, it has not been understood fully. While the opposite Thomas-Fermi limit of strong interactions has been attacked numerically, the limit we consider here is harder to be examined

[a] e-mail: georgios.kavoulakis@matfys.lth.se

numerically, since for weak interactions the numerical noise is comparable to the (very small) interaction energy. Furthermore, the diagrammatic perturbation theory developed here allows us to identify the states which contribute to the energy of the gas to first and second order. Therefore, although the results which are presented here are consistent with the ones in the Thomas-Fermi limit, they provide a more complete picture of the problem of vortex formation and vortex stability. Finally, our results are even experimentally relevant, since it is now possible to achieve the limit of weak interactions considered here.

2 Model

In our model we consider atoms interacting via a short-range effective interaction,

$$V_{\rm int} = U_0 \sum_{i \neq j} \delta(\mathbf{r}_i - \mathbf{r}_j)/2. \quad (1)$$

Here $U_0 = 4\pi\hbar^2 a/M$ is the strength of the effective two-body interaction, where a is the scattering length for elastic atom-atom collisions and M is the atom mass. We also consider a harmonic trapping potential of the form

$$V(\rho, z) = M\omega^2(\rho^2 + \lambda z^2)/2, \quad (2)$$

where ρ and z are cylindrical polar coordinates, ω is the oscillator frequency, and λ is a dimensionless constant ($\hbar = M = \omega = 1$ from now on.)

We consider weak interactions and strong confinement along the z-axis, which is taken to be the axis of rotation. For weak interactions the corresponding dimensionless quantity is $\gamma = Na/d_z$ which is our expansion parameter as it is assumed to be much smaller than unity. Here N is the total number of atoms and d_z is the oscillator length along the axis of rotation. In this limit one can work within the subspace of the nodeless ($n = 0$) eigenfunctions of the two dimensional harmonic oscillator,

$$\psi_{n,m}(\rho, \phi) = \sqrt{\frac{n!}{\pi(n+|m|)!}}\, \rho^{|m|} e^{im\phi} L_n^m(\rho^2) e^{-\rho^2/2}, \quad (3)$$

where n is the number of radial excitations, m is the quantum number of the angular momentum, and L_n^m are the associated Laguerre polynomials. More specifically, the basis states are $\psi_{0,m}(\rho, \phi) = \rho^{|m|} e^{im\phi} e^{-\rho^2/2}/\sqrt{\pi |m|!}$.

The strong confinement along the axis of rotation, $\lambda \gg 1$, implies that the cloud is in its lowest state of motion along this axis, and the problem thus becomes effectively two dimensional, as the degrees of freedom along the z-axis are frozen out. Therefore, the order parameter $\Psi(\mathbf{r})$ can be expanded in the product states $\Psi_{0,m}(\mathbf{r}) = \psi_{0,m}(\rho, \phi)\, \phi_0(z)$, where $\phi_0(z)$ is the ground state of the one dimensional harmonic oscillator.

Under the above conditions, as shown initially by Bertsch and Papenbrock [17] using numerical diagonalization, the interaction energy of the gas in the lowest state is, for $2 \leq L \leq N$,

$$\mathcal{E}_{L,N} = \gamma(N - L/2 - 1)/\sqrt{2\pi}, \quad (4)$$

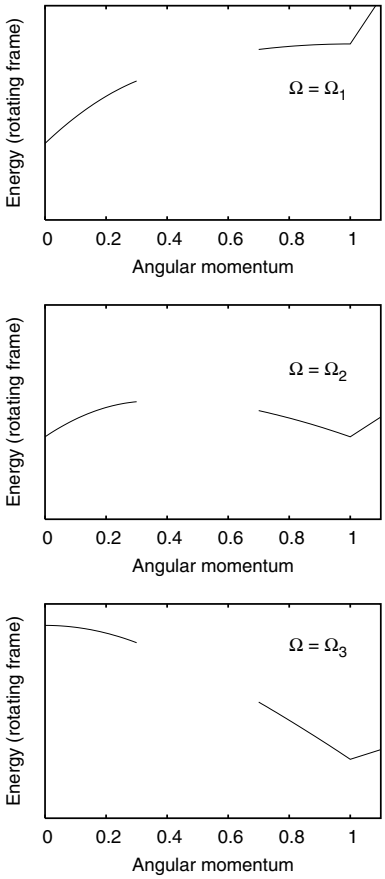

Fig. 1. Schematic diagram which shows the energy of the gas in the rotating frame as function of the angular momentum per atom l for different frequencies of rotation Ω. On the top graph, for $\Omega = \Omega_1$, the derivative of the energy at $l = 1$ vanishes. For $\Omega = \Omega_2$ the energy at $l = 0$ equals that at $l = 1$. Finally, for $\Omega = \Omega_3$ the derivative of the energy at $l = 0$ vanishes. Our study shows that $\Omega_1 < \Omega_2 < \Omega_3$, and also that the energy bents downward at both $l = 0$ and $l = 1$. All these observations have crucial consequences on the formation and stability of a single vortex state.

where L is the total angular momentum, and therefore it varies linearly with L. Reference [19] has shown analytically that this equation is *exact* to first order in γ.

Therefore, if $F = E - L\Omega$ is the total energy of the gas in the rotating frame, where $E = L + \mathcal{E}_{L,N}$ is the total energy in the rest frame then to first order in γ (henceforth the energy is measured with respect to the energy of the lowest state and terms of order $1/N$ are neglected), $F/N = (1 - \gamma/2\sqrt{2\pi} - \Omega)\, l$, where $l = L/N$. The above equation implies that the critical frequency for rotation is

$$\Omega_c^{(1)} = 1 - \gamma/2\sqrt{2\pi}. \quad (5)$$

At this value of Ω Butts and Rokhsar [14] predict that the gas undergoes a discontinuous transition from a non rotating state to a state with a vortex located at the center of the trap. In the present study we calculate the energy to next order for $0 \leq l \leq 1$ examining how this picture is modified. On the other hand, for $l > 1$ where more

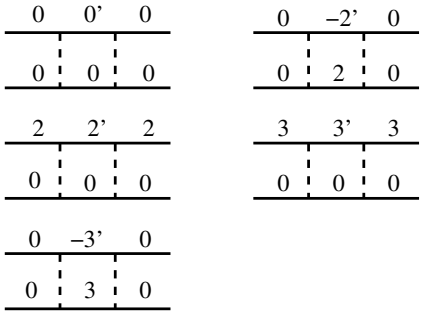

Fig. 2. The five diagrams which contribute to the energy of the gas to order γ^2 and up to $l^{3/2}$, for $1 \ll L \ll N$. The unprimed (primed) numbers denote the angular momentum m of the states with zero (any nonzero) radial excitations, $n = 0$ ($n \geq 1$). For the states with $m < 0$, n can also be zero. The dotted lines denote the interaction.

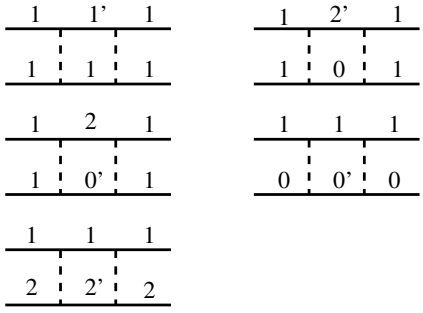

Fig. 3. The five diagrams which contribute to the energy of the gas to order γ^2 and up to l^2, for $1 \ll N - L \ll N$.

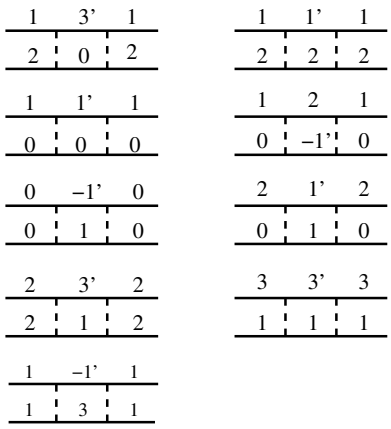

Fig. 4. The nine diagrams which contribute to the energy of the gas to order γ^2 and to l^2, for $1 \ll N - L \ll N$.

than one vortices are present, calculation of the energy to lowest order in γ suffices to determine their stability.

3 Calculation of energy in second order perturbation theory

We use now second-order perturbation theory to calculate the interaction energy to next order, i.e., to γ^2. In a similar method reference [20] has calculated the low-lying excitations of the system in the limit of low angular momentum. In our study we use the results of reference [18] which has studied both regimes of low ($1 \ll L \ll N$) and high ($1 \ll N - L \ll N$) angular momentum. Starting with $1 \ll L \ll N$, since we need both the slope, as well as the curvature of the energy (which is given by a term of order $l^{3/2}$ in this case), the order parameter is, up to the desired order,

$$\Psi = c_0 \Psi_{0,0} + c_2 \Psi_{0,2} + c_3 \Psi_{0,3}, \qquad (6)$$

where $|c_0|^2 = 1 - l/2 + l^{3/2}/3$, $|c_2|^2 = l/2 - l^{3/2}$, and $|c_3|^2 = 2l^{3/2}/3$. The five diagrams which contribute to the energy to second order in γ and up to $l^{3/2}$ are shown in Figure 2. Conservation of the angular momentum in the collisions (the interaction is spherically-symmetric) implies that the only processes which have a nonzero contribution to the energy are the ones where the angular momentum is conserved in each vertex and are shown in this figure, as well as in Figures 3 and 4.

For example, the contribution of the top left diagram to the energy per particle is equal to

$$\sum_{n=1}^{\infty} \frac{|\langle \Psi_{0,0}, \Psi_{0,0} | V_{\rm int} | \Psi_{0,0}, \Psi_{n,0} \rangle|^2}{N(\epsilon_{0,0} - \epsilon_{n,0})} = - \left(1 - l/2 + l^{3/2}/3\right)^3 (NU_0)^2 \sum_{n=1}^{\infty} \frac{|I_{0,0}^{0,n}|^2}{\epsilon_{n,0} - \epsilon_{0,0}}, \qquad (7)$$

where $I_{0,0}^{0,n} = \int \Psi_{0,0}^* \Psi_{0,0}^* \Psi_{0,0} \Psi_{n,0}\, d\mathbf{r}$ is the overlap integral between the corresponding states. This always involves three states with zero radial excitations and one state with n radial excitation(s). Also $\epsilon_{n,m} = 2n + |m| + 1 + \lambda/2$ is the eigenenergy of the states $\Psi_{n,m}(\mathbf{r}) = \psi_{n,m}(\rho, \phi)\phi_0(z)$ and $N_0 = N|c_0|^2$ is the occupancy of the state $\Psi_{0,0}$. In equation (7) there is a factor of $1/2$ from the interaction [Eq. (1)] that is cancelled by a factor of 2 that comes from the symmetrization of the wavefunction.

The sum in equation (7) is over all the excited states with $m = 0$ and $n \geq 1$ (in other cases where intermediate states with negative values of m are involved, $n \geq 0$). However, the series converges rapidly because of the overlap integrals which decrease with increasing n. Considering the first fifteen excited states, $n = 1, \ldots, 15$ we get an accuracy that is higher that machine accuracy and find that

$$E/N \approx \left(1 - \gamma/2\sqrt{2\pi}\right) l - \left(0.0916 - 0.0883\, l + 0.0156\, l^{3/2}\right) \gamma^2. \qquad (8)$$

As a final step we express E/N as function of the expectation value of the angular momentum per particle $\langle l \rangle \equiv \langle \tilde{\Psi} | \hat{L} | \tilde{\Psi} \rangle / \langle \tilde{\Psi} | \tilde{\Psi} \rangle$. Here $\tilde{\Psi} = \sum_m c_m \tilde{\Psi}_m$, with $\tilde{\Psi}_m = \Psi_{0,m} + \gamma \sum_{n \neq 0} d_{n,m} \Psi_{n,m}$ being the perturbed basis states. The corrections of order γ in the basis states introduce a correction of order γ^2 in $\langle l \rangle - l$.

To calculate $\langle l \rangle$ we start from the Gross-Pitaevskii equation and make use of the orthogonality between the

states $\Psi_{n,m}$ finding $d_{n,m} = -2\pi \int |\Psi_{0,m}|^2 \Psi_{0,m} \Psi^*_{n,m} \, d\mathbf{r}/n$. This formula implies that $\langle l \rangle = l[1 - 0.0405\,\gamma^2 - 0.0018\,\gamma^2 \, l^{1/2}]$, or $l = \langle l \rangle [1 + 0.0405\,\gamma^2 + 0.0018\,\gamma^2 \, \langle l \rangle^{1/2}]$. Combining this result with equation (8) we find

$$E/N \approx \left(1 - \gamma/2\sqrt{2\pi}\right) \langle l \rangle - \left(0.0916 - 0.1288\,\langle l \rangle + 0.0138\,\langle l \rangle^{3/2}\right) \gamma^2. \quad (9)$$

From equation (9) we conclude that the critical frequency of rotation is, to order γ^2,

$$\Omega_c^{(2)} \equiv \Omega_3 = 1 - \gamma/2\sqrt{2\pi} + 0.1288\,\gamma^2 + \mathcal{O}(\gamma^3). \quad (10)$$

Also E/N (as well as F/N) has a downward curvature.

Following a similar method we perform the same analysis for $1 \ll N - L \ll N$. There is no term of order $\tilde{l}^{3/2}$ in this case and the two leading terms are of order $\tilde{l}$ and $\tilde{l}^2$, where $\tilde{l} = 1 - l$. The corresponding order parameter is [18]

$$\Psi = c_0 \Psi_{0,0} + c_1 \Psi_{0,1} + c_2 \Psi_{0,2} + c_3 \Psi_{0,3}, \quad (11)$$

where $|c_0|^2 = 2\tilde{l} - 3\tilde{l}^2/2$, $|c_1|^2 = 1 - 3\tilde{l} + 27\tilde{l}^2/8$, $|c_2|^2 = \tilde{l} - 9\tilde{l}^2/4$, and $|c_3|^2 = 3\tilde{l}^2/8$.

The five diagrams which contribute to the interaction energy linearly and quadratically in $\tilde{l}$ are shown in Figure 3, while the ones in Figure 4 contribute only quadratically. Again, considering the first fifteen excited states we find

$$E/N \approx \left(1 - \gamma/2\sqrt{2\pi}\right)(1 - \tilde{l}) - \left(0.0111 + 0.1024\,\tilde{l} + 0.7654\,\tilde{l}^2\right) \gamma^2. \quad (12)$$

In this case $\langle \tilde{l} \rangle = \tilde{l}[1 + 0.0780\,\gamma^2 - 0.0811\,\tilde{l}\,\gamma^2]$, or $\tilde{l} = \langle \tilde{l} \rangle [1 - 0.0780\,\gamma^2 + 0.0811\,\langle \tilde{l} \rangle \, \gamma^2]$. The energy, expressed as function of $\langle \tilde{l} \rangle$ is therefore

$$E/N \approx \left(1 - \gamma/2\sqrt{2\pi}\right)\left(1 - \langle \tilde{l} \rangle\right) - \left(0.0111 + 0.0244\,\langle \tilde{l} \rangle + 0.8465\,\langle \tilde{l} \rangle^2\right) \gamma^2. \quad (13)$$

The frequency at which the derivative vanishes is thus

$$\Omega_1 = 1 - \gamma/2\sqrt{2\pi} + 0.0244\,\gamma^2 + \mathcal{O}(\gamma^3). \quad (14)$$

Again, E/N (and F/N) has a downward curvature.

Finally, another relevant frequency of rotation is the one where the energy in the rotating frame for $\langle l \rangle = 0$ equals that for $\langle l \rangle = 1$, and, in agreement with reference [21], this turns out to be

$$\Omega_2 = 1 - \gamma/2\sqrt{2\pi} + 0.0805\,\gamma^2 + \mathcal{O}(\gamma^3). \quad (15)$$

4 Discussion of the results

The angular momentum plotted on the horizontal axis of Figure 1 is directly related to the position of the vortex, since for an off-center vortex state $0 \leq l \leq 1$ [22]. Therefore, as l increases in Figure 1 the vortex moves from an infinite distance away from the trap ($l = 0$) to its center ($l = 1$). Knowing this, and having calculated the energy as function of the angular momentum in the two limiting cases, we can extract valuable information about the formation and stability of a single vortex state. Since our Hamiltonian is rotationally invariant, it commutes with the angular momentum and therefore the angular momentum is a good quantum number. In that respect, any configuration is stable, however the interesting question is the stability against weak perturbations.

For example, in the presence of a small thermal component in the gas which interacts with the condensate exchanging angular momentum and energy with it, a vortex state is stable/metastable as long as its energy in the rotating frame has an absolute/local minimum [23]. In the limit of weak interactions that we consider here, the energy is dominated by the oscillator energy and the energy barriers are small. As a result, these systems cannot support persistent currents [i.e., $F(l)$ does not have any metastable minimum at any $l \neq 0$ when $\Omega = 0$]. Still, when $\Omega \neq 0$, $F(l)$ develops in principle local minima and in what follows, we consider a vortex state as a stable configuration provided that $F(l)$ has a local/absolute minimum (henceforth l is to be identified as $\langle l \rangle$).

Our results here are exact for weak interactions and for values of the angular momentum close to zero and unity (note that analytic expansions of the energy are possible only in these two limits). Still, our expansion strongly suggests that the schematic form of $F(l)$ shown in Figure 1 extends over all the intermediate values of the angular momentum, without any local minima in between.

As shown in Figure 1 for any frequency Ω between Ω_1 and Ω_2, $F(l)$ has a local minimum at $l = 1$. In other words a vortex that is located at the center of the trap first becomes stable locally with increasing Ω. This behavior is qualitatively the same as in reference [16] where the opposite limit of strong interaction was considered. As shown in the same graph, the slope of $F(l)$ increases discontinuously as one crosses the point $l = 1$. This increase is on the order of γ, equal to $11\gamma/32\sqrt{2\pi}$ [18]. This fact guarantees that $F(l)$ has a local/absolute minimum at $l = 1$ for all values of Ω between Ω_1 and Ω_3.

According to our study, if one first cools down below the condensation temperature and then rotates, the gas will undergo a discontinuous transition from a non-rotating state to a state with a vortex in the middle of the cloud for $\Omega = \Omega_3$. In the reverse process as Ω decreases, the gas will make a discontinuous transition from $l = 1$ to $l = 0$ at an $\Omega = \Omega_1$, with $\Omega_1 < \Omega_3$. In the other physically-relevant situation, if one first rotates with some $\Omega = \Omega_0$ and then cools down below the condensation temperature, the gas may actually reach the state with a (stable) centered vortex for any value of Ω_0 between Ω_1 and Ω_3.

The author thanks Nikos Papanicolaou for suggesting this problem to him and for useful discussions. He also thanks the Physics department of the university of Crete for its hospitality. This work was supported by the Swedish Research Council (VR), and by the Swedish Foundation for Strategic Research (SSF).

References

1. M.R. Matthews et al., Phys. Rev. Lett. **83**, 2498 (1999)
2. K.W. Madison et al., Phys. Rev. Lett. **84**, 806 (2000); F. Chevy et al., Phys. Rev. Lett. **85**, 2223 (2000); K.W. Madison et al., Phys. Rev. Lett. **86**, (2001)
3. J.R. Abo-Shaeer et al., Science **292**, 476 (2001)
4. P.C. Haljan et al., Phys. Rev. Lett. **87**, 210403 (2001); P. Engels et al., Phys. Rev. Lett. **89**, 100403 (2002)
5. F. Dalfovo, S. Stringari, Phys. Rev. A **53**, 2477 (1996)
6. R.J. Dodd et al., Phys. Rev. A **56**, 587 (1997)
7. D.S. Rokhsar, Phys. Rev. Lett. **79**, 2164 (1997)
8. A.A. Svidzinsky, A.L. Fetter, Phys. Rev. A **58**, 3168 (1998)
9. A.A. Svidzinsky, A.L. Fetter, Phys. Rev. Lett. **84**, 5919 (2000)
10. H. Pu et al., Phys. Rev. A. **59**, 1533 (1999)
11. T. Isoshima, K. Machida, J. Phys. Soc. Jpn **68**, 487 (1999)
12. J.J. García-Ripoll, V.M. Pérez-García, Phys. Rev. A **60**, 4864 (1999)
13. D.L. Feder et al., Phys. Rev. Lett. **82**, 4956 (1999)
14. D.A. Butts, D.S. Rokhsar, Nature **397**, 327 (1999)
15. J.J. García-Ripoll, V.M. Pérez-García, Phys. Rev. A **63**, 041603(R) (2001)
16. T. Isoshima, K. Machida, Phys. Rev. A **60**, 3313 (2003)
17. G.F. Bertsch, T. Papenbrock, Phys. Rev. Lett. **83**, 5412 (1999)
18. G.M. Kavoulakis et al., Phys. Rev. A **62**, 063605 (2000)
19. A.D. Jackson, G.M. Kavoulakis, Phys. Rev. Lett. **85**, 2854 (2000); R.A. Smith, N.K. Wilkin, Phys. Rev. A **62**, 061602 (2000); T. Papenbrock, G.F. Bertsch, Phys. Rev. A **63**, 023616 (2001)
20. G.M. Kavoulakis et al., Phys. Rev. A **63**, 055602 (2001)
21. M. Linn, A.L. Fetter, Phys. Rev. A **60**, 4910 (1999)
22. C.J. Pethick, H. Smith, *Bose-Einstein Condensation in Dilute Gases* (Cambridge University Press, 2002)
23. A.J. Leggett, Rev. Mod. Phys. **73**, 307 (2001)